3056–3067 *Nucleic Acids Research, 2013, Vol. 41, No. 5* *Published online 18 January 2013*
doi:10.1093/nar/gks1459

Spontaneous telomere to telomere fusions occur in unperturbed fission yeast cells

Hugo Almeida and Miguel Godinho Ferreira*

Instituto Gulbenkian de Ciência, Rua da Quinta Grande 6, 2780-156 Oeiras, Portugal

Received November 14, 2012; Revised December 13, 2012; Accepted December 14, 2012

ABSTRACT

Telomeres protect eukaryotic chromosomes from illegitimate end-to-end fusions. When this function fails, dicentric chromosomes are formed, triggering breakage-fusion-bridge cycles and genome instability. How efficient is this protection mechanism in normal cells is not fully understood. We created a positive selection assay aimed at capturing chromosome-end fusions in *Schizosaccharomyces pombe*. We placed telomere sequences with a head to head arrangement in an intron of a selectable marker contained on a plasmid. By linearizing the plasmid between the telomere sequences, we generated a stable mini-chromosome that fails to express the reporter gene. Whenever the ends of the mini-chromosome join, the marker gene is reconstituted and fusions are captured by direct selection. Using telomerase mutants, we recovered several fusion events that lacked telomere sequences. The end-joining reaction involved specific homologous subtelomeric sequences capable of forming hairpins, suggestive of ssDNA stabilization prior to fusing. These events occurred via microhomology-mediated end-joining (MMEJ)/single-strand annealing (SSA) repair and also required MRN/Ctp1. Strikingly, we were able to capture spontaneous telomere-to-telomere fusions in unperturbed cells. Similar to disruption of the telomere regulator Taz1/TRF2, end-joining reactions occurred via non-homologous end-joining (NHEJ) repair. Thus, telomeres undergo fusions prior to becoming critically short, possibly through transient deprotection. These dysfunction events induce chromosome instability and may underlie early tumourigenesis.

INTRODUCTION

The ends of eukaryotic chromosomes prevent DNA double-strand break (DSB) repair through a specialized protective structure called the telomere. Telomeres are composed of G-rich DNA repeats bound by a protein complex known as shelterin (1,2). In the absence of shelterin, telomeres undergo end-to-end fusions that give rise to genomic instability (3–5). Several studies suggest that genomic instability initiated by telomere dysfunction may underlie carcinogenesis (6).

The functions of telomere protection have been dissected in several organisms from yeast to humans. One major function is to compensate for the incomplete replication of the ends of chromosomes, known as the 'end replication problem' (7). This is generally achieved by telomerase, a reverse transcriptase that adds new telomere repeats to the ends of chromosomes (8–10). In the fission yeast *Schizosaccharomyces pombe*, telomere elongation by telomerase is regulated by Taz1, orthologue of both human TRF1 and TRF2, also involved in chromosome-end protection (2,11,12). In absence of Taz1, telomere-to-telomere fusions occur via non-homologous end-joining (NHEJ) repair, a mode of DSB repair up-regulated in the G1 phase of the cell cycle (2,11,12). Similarly, disruption of either human TRF2 or budding yeast Rap1 results in telomere-to-telomere fusions perpetrated by NHEJ repair (13,14). During DNA replication, the replication fork unwinds the telomere and exposes chromosome ends. While this permits the engagement of telomerase, it also causes momentarily deprotection that triggers DNA damage checkpoints (15,16).

Although loss of the telomere repeat factor Taz1 triggers NHEJ-mediated fusions, erosion of telomeric DNA leads to a different mode of DNA repair. In the absence of telomerase, Stn1, Ten1 or Pot1—components that protect the 3′-overhangs from degradation (17)—chromosome ends undergo fusions through a DNA repair process that requires exposure of complementary ssDNA regions on both DNA ends (18). Depending on the size of the homology region involved, this process has been termed single-strand annealing (SSA) or microhomology-mediated end-joining (MMEJ) repair (19). In fission yeast, these fusions normally occur 7–13 kb internally after complete disappearance of telomere sequences (20). In mouse cells, a microhomology-dependent mechanism of DNA repair termed A-NHEJ also mediates fusions after

*To whom correspondence should be addressed. Tel: +351 21 446 4654; Fax: +351 21 440 7970; Email: mgferreira@igc.gulbenkian.pt

removal of Pot1a/b-Tpp1 (21). Similar results were obtained for fusions observed in telomerase-deficient budding yeast and mice models (3,22). Chromosome-end fusions were also observed in telomerase-positive human cell lines (23). Most involve critically short telomeres, suggesting that telomeres fuse after eroding past a minimum length required for protection. In contrast to these studies, wild-type length telomeres can engage end fusions. Gottschling and colleagues used a positive selection assay in budding yeast based on an induced DSB and observed extremely rare telomere-to-DSB fusions in WT cells, highlighting that normal telomeres are protected from engaging in NHEJ repair with other DNA breaks (24).

Here we investigate the nature of telomere protection in fission yeast using a novel quantitative telomere fusion assay. We find that telomerase mutants show microhomology-dependent fusions possibly mediated by transient DNA hairpin structures. In contrast to previous observations, we show that wild-type telomeres are subjected to spontaneous fusions via NHEJ, which do not require critical telomere shortening. Thus, functional telomeres can be involved in spontaneous telomere fusions, which may trigger genomic instability preceding carcinogenesis.

MATERIALS AND METHODS

Mini-chromosome and plasmid construction

pFT2

The *his3*$^+$ gene was cloned into pBluescriptII KS(+) using a blunt-ended NotI/SmaI digestion. A synthetic 100 mer oligonucleotide containing subtelomeric sequences in a head-to-head orientation, derived from the pNSU70 plasmid (25) separated by an ApaI restriction fragment was cloned into the XbaI restriction site of *his3*$^+$. The resulting *his3*$^+$ fragment was then removed from pBluescriptII using PstI and SacI and cloned into the PstI and SacI sites of pREP3X. The SacI site was subsequently destroyed by digestion and blunt-end ligation to generate pREP-his-telo. Subsequently, an ApaI restriction fragment containing opposing telomere sequences separated by an *Escherichia coli* kanR resistance gene was derived from the pEN53 plasmid (26) and cloned into the ApaI site, thus spacing the subtelomeric sequences of pREP3X-his-telo to give pFT2. Linearization of the plasmid was achieved by removing the SacI-enclosed kanR sequence in between the telomere sequences.

pREP-his3$^+$

The *his3*$^+$ gene was cloned into pREP3X using PstI and SacI sites to generate pREP-*his3*$^+$.

pREP42-taz1$^+$

pREP42- *taz1*$^+$ was used in the construction of the taz1+ o/e strain. The *taz1*$^+$ORF was cloned in a pTOPO vector (Invitrogen). pTOPO was then digested with BamHI and SalI and the resulting *taz1*$^+$fragment was cloned into the BamHI and SalI sites of pREP42 vector.

Media and genetic methods

We used standard recipes for Yeast Extract with supplements (YES) and Edinburgh minimal medium (EMM) as described in (27). Methods of transformation, sporulation and tetrad dissection are described in (27–29).

Strains

Strains used in this study are described in Supplementary Table S1. Lines derived from genetic crosses are indicated in the parental column with both parental strains indicated. All deletions were performed using the procedures described in (28).

taz1$^+$ *o/e*

To create strain MGF1898, pREP42-*taz1*$^+$ was digested with KpnI and transformed for integration. Insertion at the *taz1*$^+$ locus was confirmed by PCR.

Primers

Primers used for amplification and sequencing of captured fusions were as follows: 495:GAACTTCAGCCTTATCG CTG; 496: CCACGGAAATAACCGAACCA; 613: GGG TAATAATTGATATGAGGGC; 614: CCACGGAAAT AACCGAACCA. Primers used for confirmation of insertion of pREP42-*taz1*$^+$ fragment at the *taz1*$^+$ locus were as follows: 178: TTCGCCTCGACATCATCTGC; 375: CCTCAGTGGCAAATCCTAAC; 711: TCTTTTACAG TTTCCTTCCC; 717:ATTGCAGAGTAAACACGACG; 736: TGGACTTTGCGTATGAGACG.

Serial dilution assays

Cultures were grown at 32°C to logarithmic phase and re-suspended to a cell density of 1×10^7 cells/ml. Ten-fold serial dilutions were performed in EMM media, and 5 µl of each dilution were spotted onto EMM plates with the described supplements and incubated at 32°C up to 7 days.

Telomere fusion assays

Cultures were grown at 32°C to logarithmic phase in EMM media containing Leucine and plated on solid EMM media containing Leucine ± Histidine. Plates were incubated at 32°C up to 7 days and colonies were counted. For time course experiments, cultures were diluted at each time point to 5×10^5 cells/ml and incubated the appropriate times in EMM media containing Leucine ± Histidine.

Western blotting

Cells were lysed in 20% TCA and the resulting protein extracts were resolved by SDS-PAGE, transferred to PVDF membranes (GE Healthcare RPN203D) and probed with primary α-Taz1 antibody (a gift from Julia P. Cooper). After incubation with HRP-conjugated secondary antibodies (GE Healthcare NA934), bands were visualized using ECLPlus (GE Healthcare RPN2132) in a STORM scanner (Amersham). Quantification was performed using ImageJ software.

Southern blotting

Genomic DNA was obtained from exponentially growing cells in YES or EMM media with supplements, using the phenolic extraction method described (27) and digested with the appropriate restriction enzymes. Southern blot analysis was performed as described (10). Briefly, DNA was separated in 0.8% agarose gels and transferred by capillarity to genomic blotting membranes (Bio-Rad, #162-0196). The DNA was then cross-linked using UV radiation and the membranes were hybridized using Church–Gilbert solution at 65°C. An overnight incubation was performed with a telomere repeat probe or a *rad4*$^{+}$ genomic probe labelled with ^{32}P using the Prime-it II random primer labeling kit (Stratagene). The membrane was washed for 30 min at 65°C with a 1× SSC 1% SDS solution and exposed to a PhosphoImager screen (Amersham) for 1–3 days depending on signal strength. The PhosphoImager screen was scanned with a STORM scanner (Amersham). Telomere length was calculated by normalizing molecular weight with telomere signal intensity, as described in (30). Number of pFT2 copies per cell was calculated by dividing signal intensity from *ars1* fragment present in pFT2 with the signal intensity from the endogenous *ars1*. This number was multiplied by a factor of 0.3 to account for the measured fraction of cells in a population under selection for *LEU2* harbouring pFT2 (See Supplementary Figure S2).

PCR reactions

Mini-chromosome end fusions were amplified by PCR. Forward primers (495: GAACTTCAGCCTTATCGC TG; 613:GGGTAATAATTGATATGAGGGC) were used for promoter proximal sequencing and the reverse primers (496:CCACGGAAATAACCGAACCA; 614:CCACGGAAATAACCGAACCA) for terminator proximal sequencing.

RESULTS

Direct assay to capture telomere fusions

To devise a scheme to detect telomere fusions, we resorted to the ability of introns to bear gene-unrelated sequences, such as telomeres. We cloned the *his3*$^{+}$ gene in a fission yeast plasmid carrying a *LEU2* marker, allowing for double selection in media lacking both histidine and leucine. Subsequently, we introduced two telomeres of 258 bp in a head to head arrangement in a unique site of the second intron of *his3*$^{+}$ thus creating pFT2 (Figure 1A). These telomeres were flanked by 80 bp of subtelomeric sequences on each side. The telomere sequences did not impair *his3*$^{+}$ expression and allowed for growth in media lacking both leucine and histidine (pFT2-Cir, Figure 1B). We then linearized pFT2 between the telomere sequences and transformed WT cells, thus creating a mini-chromosome in which the *his3*$^{+}$ gene was split between the two extremities of the plasmid (Figure 1A). Consequently, the linear mini-chromosome pFT2 could be maintained through selection using *LEU2* expression but was now unable to grow on media lacking histidine (pFT2-Lin, Figure 1B). We reasoned that any event that would disrupt telomere protection leading to plasmid end joining would restore the initial circular configuration of pFT2 and allow for *his3*$^{+}$ expression. We also asserted that intron length would not be limiting in our assay by observing the unimpaired growth of strains harbouring circular pFT2 carrying a 1.3 kbp Kan^{r} cassete in the *his3*$^{+}$ intron (data not shown). As long as the *his3*$^{+}$-coding sequence is not eroded, this system identifies any type of end joining to occur between the ends of the mini-chromosome, as introns do not rely on a coding reading frame.

We next gathered evidence that the mini-chromosome was propagated linearly in cells and that telomeres were functional. We produced genomic DNA from fission yeast cells and digested it with either EcoRV that would release the *his3*$^{+}$ promoter proximal telomere (T Prom) or XhoI that cuts near the *his3*$^{+}$ terminator, generating a fragment containing the terminator proximal telomere (T Term; Supplementary Figure S1). We next performed Southern blotting using a telomere probe that revealed the telomere sequences present in the cell's chromosomes and in the newly generated mini-chromosome (Figure 1C). Both chromosome ends showed a distribution of sizes typical of telomeres, suggesting that the ends of the mini-chromosome were free and were being used as a substrate by telomerase.

To test the mini-chromosome stability and to confirm that it was independent of the remaining chromosomes, we analysed the ability of these cells to lose pFT2 in either the linear or the circular form. Cells were grown in media containing leucine and histidine for several generations and then tested for the ability to retain pFT2. Fission yeast plasmids lack centromeric sequences and are thus missegregated and lost when not under selection (31). We confirmed that pFT2 either in the circular or linear configuration were lost at a similar rate as other plasmids (Supplementary Figure S2). Thus, our mini-chromosome was maintained independently of the remaining genome, showing that its telomeres were able to recruit telomerase and protect its ends.

We wanted to know whether we could use our assay to analyse chromosome-end fusions. As a proof of principle, we crossed an early generation telomerase mutant with the strain harbouring the pFT2 mini-chromosome and allowed the progeny to undergo telomere erosion over several days. On each time point, we collected samples for Southern blotting and plated cells on media containing and lacking histidine to measure the ability to fuse the ends of the mini-chromosome. Using a telomere probe, we could observe the slow erosion of telomeres in *trt1*Δ mutants over several days (Figure 1D). Throughout this experiment, control WT did not generate detectable colonies in histidine-depleted media (Figure 1E). However, by day 6, coincident with the lowest signal for the mini-chromosome telomeres, *trt1*Δ cells showed a steadily increase in *his3*$^{+}$-expressing cells. Over the course of the experiment, productive mini-chromosome fusions increased to represent 5–8% of all the cells harbouring the pFT2 plasmid. Given that several mini-chromosome fusions are likely to occur in a way

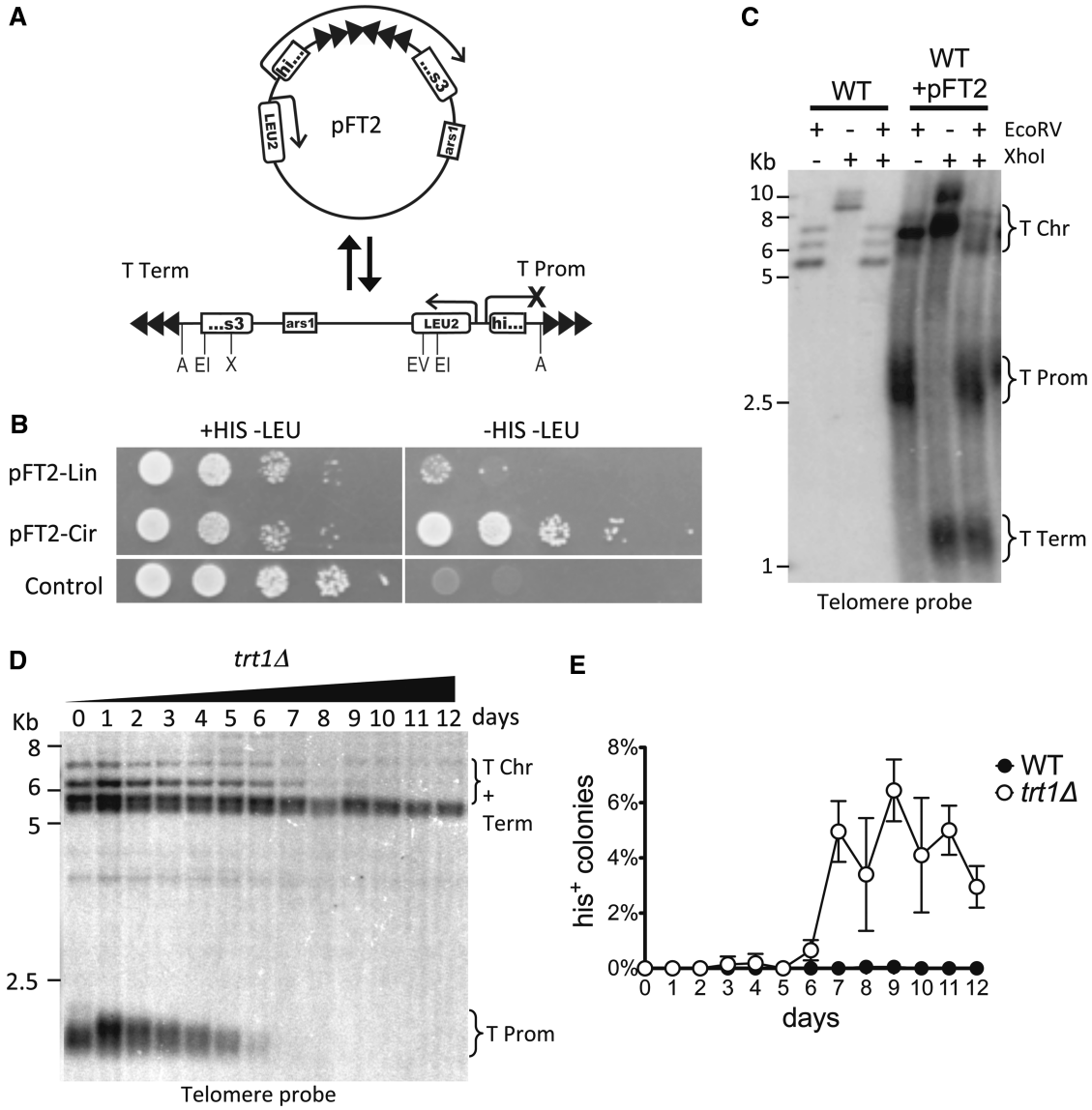

Figure 1. Mini-chromosome assay used to detect telomere fusions. (**A**) Fusion of both ends of the linear pFT2 mini-chromosome generates a circular plasmid that expresses the *his3*$^{+}$ gene. Relevant restriction sites are indicated as follows: A—ApaI; EI—EcoRI; EV—EcoRV; X—XhoI. (**B**) Ten-fold serial dilutions of WT cells carrying either the linear (pFT2-Lin) or circular (pFT2-Cir) mini-chromosome plated on permissive (+HIS −LEU) or restrictive (−HIS −LEU) media. Control cells contain a *LEU2*-based plasmid that lacks the *his3*$^{+}$ gene. (**C**) Southern blot analysis of telomeres in a WT strain harbouring pFT2. Genomic DNA extracts were digested with EcoRV and/or XhoI enzymes and probed for telomeres (see Supplementary Figure S1 for details). Promoter-proximal (T Prom), terminator-proximal telomeres (T Term) and chromosomal telomeres (T Chr) are depicted. (**D**) Southern blot analysis of telomere shortening in a *trt1*Δ strain. Cells were grown in liquid culture and genomic DNA extracts were digested with EcoRV. (**E**) Frequency of WT and *trt1*Δ strains able to express histidine. Percentages were calculated by dividing the number of colonies growing in +HIS −LEU and −HIS −LEU. Error bars represent SEM of three replicates for each time point.

that fail to reconstitute *his3*$^{+}$ expression, we anticipate that we are under-estimating the whole population of fusions.

Taz1 levels are limiting to control telomere length

We wanted to define the impact for the cell to harbour more telomeres than the ones it usually carries. Haploid fission yeast contains three chromosomes and spends most of its cell cycle in S/G2 phases. Thus, cells carry a maximum of 12 telomeres at any given time. Introducing several other telomeres could alter telomere dynamics. To investigate the impact of extra telomeres per cell, we first quantified how many mini-chromosomes would a cell carry on average. We used Southern blot analysis to quantify the *ars1* fragments, which are present as a single copy both in the genome and in the mini-chromosome (Supplementary Figure S3). Given that not all cells in the population carry a mini-chromosome due to natural plasmid loss, even when under selection, we calculated that the mini-chromosomes would be in a range of 5–7 copies per cell, thus increasing the overall number of telomeres.

To assess the impact of extra copies of telomeres, we looked at telomere length in cells carrying the

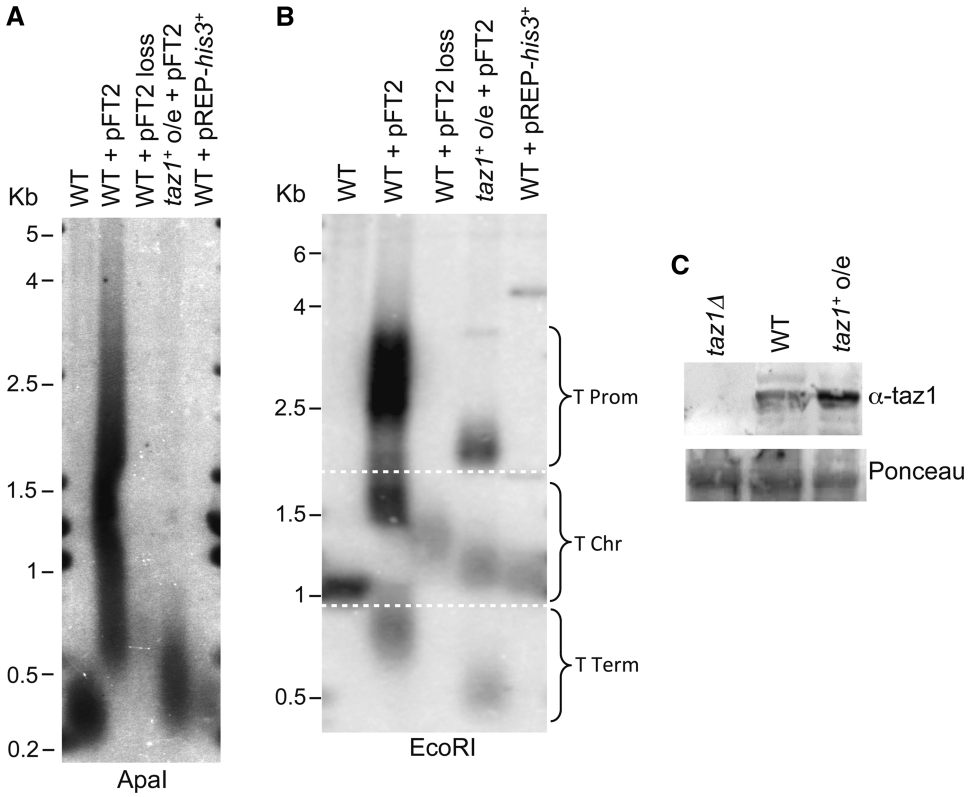

Figure 2. Linear mini-chromosomes affect telomere length through dilution of Taz1 (**A**) Southern blot analysis of telomere length in WT strains carrying pFT2, after pFT2 loss and with taz1$^+$ o/e. Genomic DNA extracts were digested with ApaI and probed for telomere DNA. ApaI digestion does not discriminate between endogenous and pFT2 telomere ends. (**B**) The same genomic DNA extracts analysed in (A) were digested with EcoRI and probed for telomere DNA. EcoRI digests separate the chromosomal telomeres (≈1 Kb) from the mini-chromosome telomeres. (**C**) Over-expression of Taz1 was monitored on a western blot using α-taz1 (top) and Ponceau staining as loading control (bottom).

mini-chromosome and compared to control cells. Using an ApaI restriction enzyme that is unable to discriminate the source of the telomeres analysed, we observed that the presence of the mini-chromosome gives rise to a 3- to 5-fold increase in overall telomere length (Figure 2A, lane 2). We then used an EcoRI digest to discriminate between the chromosome telomeres and those harboured in the mini-chromosome. Southern blots verified that the chromosome telomeres were elongated in cells carrying the mini-chromosome (Figure 2B, lane 2). The mini-chromosome was the cause for the changes in telomere length, since telomere length decreased in cells that lost the linear plasmid (Figure 2B, lane 3). The same increase was observed in a strain carrying a circular configuration of the mini-chromosome (Supplementary Figure S4B). Thus, as a consequence of increasing the number of telomeres in the cell, the overall telomere length is increased, suggesting the titration of a limiting factor that controls telomere length.

We aimed at having a plasmid fusion assay that mimics WT cells as close as possible. Even though there is no indication that small variation in length, such as the one observed, results in deficiencies in telomere protection, we set up to identify the possible regulator of telomere length that was limiting. Using plasmids carrying the *nmt1*$^+$ promoter, we independently over-expressed Taz1, Rap1, Pot1 and Ccq1 in cells carrying the mini-chromosome (data not shown). Only Taz1 over-expression resulted in an almost complete reduction of telomere length to wild-type length of all telomeres. The same result was observed when we integrated a Taz1 over-expression cassette in the genome of a strain, to which we called *taz1*$^+$ *o/e* (Figure 2B). This strain was used in all remaining experiments. By western blotting, we estimated that Taz1 was over-expressed about 2-fold when compared with WT levels (Figure 2C). Thus, levels of the telomere binding Taz1 are limiting in fission yeast and, when telomere number increases, this results in net telomere elongation. Accordingly, budding yeast's telomere-binding factor Rap1 was also limiting upon increase in telomere numbers (32,33).

*trt1*Δ mini-chromosome fusions are MRN dependent and occur via SSA/MMEJ repair

Capturing telomere fusions residing on a plasmid allows us to study not only their abundance but also the mechanism whereby they arise. Previous studies revealed that chromosome-end fusions in *trt1*Δ in fission yeast were a consequence of the *rad16*$^+$ (*ScRAD1* and mammalian XPF)-dependent SSA/MMEJ pathway (18). To test the genetic requirements for mini-chromosome fusions, we produced *trt1*Δ mutants in which we deleted specific key factors regulating different DNA repair pathways. We allowed *trt1*Δ, *trt1*Δ *rad16*Δ and *trt1*Δ *lig4*Δ mutants

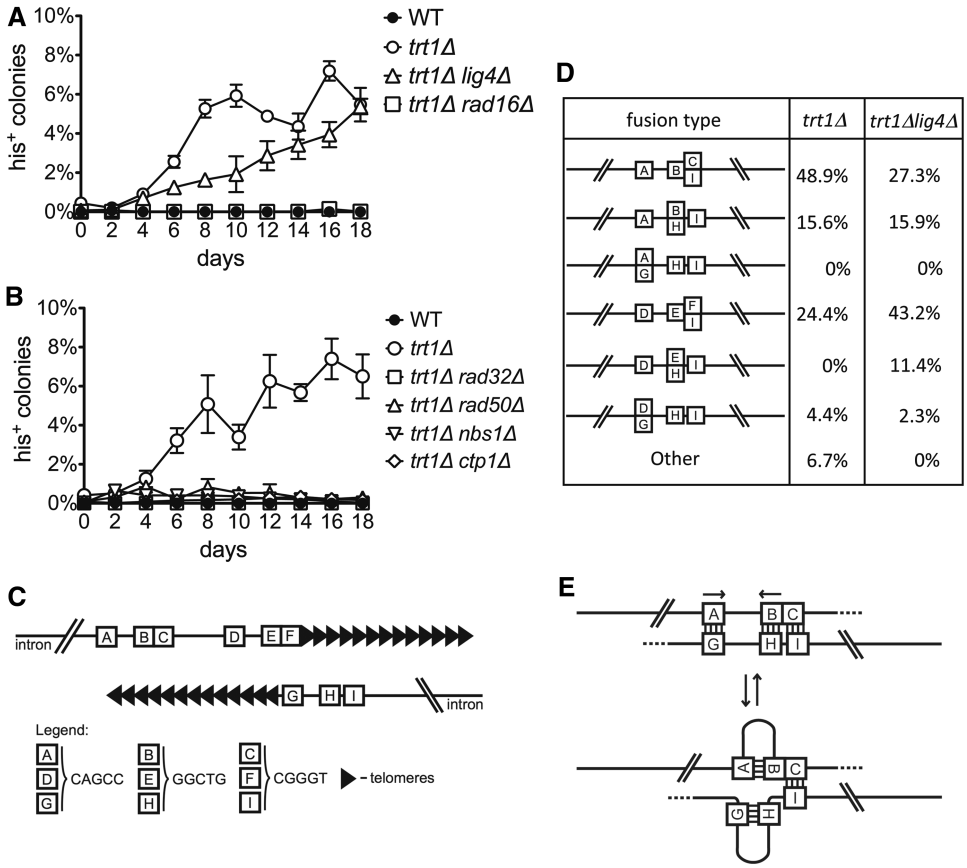

Figure 3. Mini-chromosome fusions in *trt1*Δ occur via *rad16*-dependent SSA/MMEJ repair and require MRN/Ctp1. (**A**) Expression of histidine during telomere erosion in *trt1*Δ, *trt1*Δ *lig4*Δ and trt1Δ *rad16*Δ strains. (**B**) Expression of histidine during telomere erosion in *trt1*Δ, *trt1*Δ *MRN*Δ and *trt1*Δ *ctp1*Δ strains. Cells were plated daily on +HIS −LEU and −HIS −LEU media. Frequencies for (A) and (B) were calculated by dividing the number of colonies growing in +HIS −LEU and −HIS −LEU. Error bars represent SEM of three replicates for each time point. (**C**) Schematic representation of the 5 nt microhomologies found at the fusion junctions in *trt1*Δ and *trt1*Δ *lig4*Δ strains. (**D**) Frequency of each microhomology at fusion junctions. *trt1*Δ strain, $n = 45$; *trt1*Δ *lig4*Δ strain, $n = 44$. (**E**) A model for microhomology-mediated fusions in *trt1*Δ and *trt1*Δ *lig4*Δ strains.

carrying the mini-chromosome to undergo telomere erosion and quantified the number of colonies expressing histidine as a measure of end-joining events. Both *trt1*Δ and *trt1*Δ *lig4*Δ mutants produced substantial mini-chromosome fusions (Figure 3A). This was consistent with previous observations (34), in which Lig4-dependent NHEJ repair was dispensable for generating *trt1*Δ survivors in fission yeast. In contrast, *rad16*$^+$ was required for *trt1*Δ mini-chromosome end fusions (Figure 3A). These results demonstrate not only that the SSA/MMEJ pathway is required for joining the ends of the mini-chromosome, but also that the repair mechanisms triggered on chromosomes are the ones responsible for repairing the ends present in the mini-chromosome, thus validating our assay.

In parallel, we investigated the role of MRN (Rad32/Rad50/Nbs1)/Ctp1 (MRX/*ScSAE2* or mammalian MRN/CtIP) in generating mini-chromosome end fusions in *trt1*Δ mutants. For this purpose, we established mutants of each component of this complex and conjugated them in a *trt1*Δ background. Absence of MRN/Ctp1 also failed to produce *trt1*Δ survivors capable of expressing histidine (Figure 3B). Thus, MRN and its nuclease partner Ctp1 are required to process mini-chromosome ends for the SSA/MMEJ repair reaction.

In contrast to TRF2 and *taz1*Δ mutants, chromosome-end fusions in *trt1*Δ mutants occurred only after total telomere erosion. We set out to investigate the sequences present at the junction of the mini-chromosome. We devised PCR reactions with primers on each side of the intron and verified that all of the *trt1*Δ histidine-producing cells possessed an intact *his3*$^+$ intron ($n = 45$), denoting that they occurred between the cloned subtelomeric sequences of the mini-chromosome. We sequenced *trt1*Δ and *trt1*Δ *lig4*Δ fusion junctions and, to our surprise, >90% involved a set of three pentanucleotide G-rich sequences present within the 85 bp subtelomeric region (Figure 3C and D). Consistent to what was previously reported (3,20,22), all but one of the *trt1*Δ fusions involved telomere sequences. The pentanucleotide sequences were arranged in a direct repeat spanning 30 bp and were present at both ends of the mini-chromosome (Figure 3C, Supplementary Figure S5), two promoter proximal (depicted as ABC and DEF) and one terminator proximal (GHI).

Not all pentanucleotides were equally involved in fusions, and there was a clear preference for those with C/I and F/I pairs (73.3% and 70.5% in *trt1*Δ and *trt1*Δ *lig4*Δ, respectively, Figure 3D). We wondered why fusions comprising the pentanucleotide present in C, F and I were

dominant. We realized that the remaining other two pentanucleotides formed an inverted repeat spaced by 14 bp that could be engaged in a hairpin structure (Figure 3E). Conceivably, as telomeres erode, ssDNA is generated at subtelomeric regions of the mini-chromosome creating the opportunity for secondary DNA structures such as hairpins. This may momentarily stabilize the sequences involved in the hairpin, thus exposing the adjacent pentanucleotide for SSA/MMEJ repair. This model is consistent with the requirement of MRN/Ctp1 in *trt1*Δ fusions, since the complex would be engaged in processing the hairpin as part of the DNA repair reaction (35,36).

Telomere–telomere fusions occur in unperturbed WT cells via NHEJ repair

As we generated our telomere fusion assay, we wondered about the rare colonies appearing in unperturbed WT cells grown on media lacking histidine (Figure 1B). These escapers originated from previous cells that carried the linear mini-chromosome and did not express *his3*$^+$, suggesting that they were the outcome of unsuspected fusions taking place in unperturbed cells. We measured the frequency of these events. In *taz1*$^+$ *o/e* cells, the frequency of colonies expressing *his3*$^+$ was $1.4 \times 10^{-4} \pm 0.5 \times 10^{-4}$ (SEM, $n = 3$; Figure 4A). In contrast, cells with longer telomeres in which Taz1 was limiting had a higher reversion frequency of $3.4 \times 10^{-4} \pm 0.9 \times 10^{-4}$ (SEM, $n = 3$), suggesting that insufficient Taz1 levels to maintain normal telomere length also resulted in reduced protection from end fusions.

Chromosome-end fusions in unperturbed cells expressing telomerase were previously reported in transformed human cell lines (23). These were the result of completely eroded telomeres fusing to a shorter telomere involving microhomologies at the junction. To identify the mechanism behind our mini-chromosome fusions, we first investigated the genetic requirements underlying these events. As previously, we deleted the genes involved in cells containing the mini-chromosome and quantified the ability of expressing the *his3*$^+$ reporter gene. In contrast to the observed mini-chromosome fusions in *trt1*Δ survivors, *rad16*$^+$-dependent SSA/MMEJ repair is dispensable in *taz1*$^+$ o/e (Figure 4A). However, mutations in key elements of the NHEJ pathway, such as *pku70*Δ and *lig4*Δ, reduced the number of *his3*$^+$-expressing colonies about 10-fold (Figure 4A). These results indicate that end-fusions occurring in unperturbed cells are processed by a distinct pathway to the ones caused by gradual telomere erosion, suggesting that they are fundamentally different uncapping events.

We next asked whether MRN/Ctp1 was required for NHEJ-mediated fusions of mini-chromosome ends. In contrast to budding yeast, MRN is dispensable for NHEJ repair in *S. pombe* as measured on plasmid-based assays (37). Surprisingly, mutants in all subunits of MRN, including Ctp1, were deficient in joining the two ends of the mini-chromosome by NHEJ repair (Figure 4B). Our data suggests that, in contrast to NHEJ measured in naked plasmid ends, MRN/Ctp1 is required to process mini-chromosome ends before undergoing end-joining reactions.

The requirement of NHEJ repair for chromosome fusions in unperturbed cells suggested that a different event occurred at the ends of our mini-chromosome. To attempt at identifying the incident that originated the end-fusion, we sequenced the junction at *his3*$^+$ mini-chromosomes. Almost all fusion events involved two telomeres on each side of the junction (89.3%, $n = 28$; Figure 4C and D and Supplementary Figure S6). The remaining involved one telomere and a subtelomere or two subtelomeres (7.1% and 3.6%, respectively). In all cases, we did not observe clear microhomologies at the junction, even though fusions often involve guanidine bases, as expected from G-rich telomere sequences (data not shown). Thus, in contrast to the previous studies in immortalized humans cell lines (23), our data suggest that uncapping events occur at telomere sequences that result in end-fusions via NHEJ repair.

Telomere fusions occur between half-sized telomeres

Even though mini-chromosome fusions exhibited substantial telomere sequences in a head to head arrangement, it was not clear whether the end-joining event resulted from one of them being too short to sustain telomere protection. To investigate the telomere length distribution in fusions, we organized telomeres in a length histogram (Figure 5A). There was a 2-fold size difference between the median telomere size at T Prom and T Term (T Prom 232 bp and T Term 111 bp; interquartile range (IQR) 92–291 bp and 29–147 bp, respectively). This was consistent with the average telomere lengths exhibited by the mini-chromosome, as analysed by Southern blot (T Prom 415 bp and T Term 184 bp, Figure 2A and B). Interestingly, a 2-fold difference between the size of T Term and T prom was also observed for the strain with deficient Taz1 levels (Figure 2B, lane 2). Thus, even though the methods used provide measures of different accuracy, our data suggest that most fusions occur between telomeres of about half the normal length observed in the linear configuration.

The difference in length between the promoter and terminator telomeres could arise due to a telomerase preference for one telomere over the other. This preference may reflect transcription of both the T Prom and endogenous telomeres, either through *his3*$^+$ or TERRA transcription, which does not occur at the T Term telomere. To discriminate whether one telomere was more frequently engaged by telomerase over the other, we compared the degenerated telomere sequences of fission yeast present at fusion junctions. As in most yeast species, *S. pombe* telomerase is 'faulty' providing other nucleotides in between the consensus $(GGTTAC)_n$. This property allowed us to recognize the original telomere sequence and identify how much erosion telomeres suffered and which new sequences were added (Figure 5B). We suggest that telomerase has a preference for T Prom since it had added repeats to most telomeres engaged in fusions (26/28). In contrast, only about half of the T Term telomeres have new sequences added (16/28). As a result,

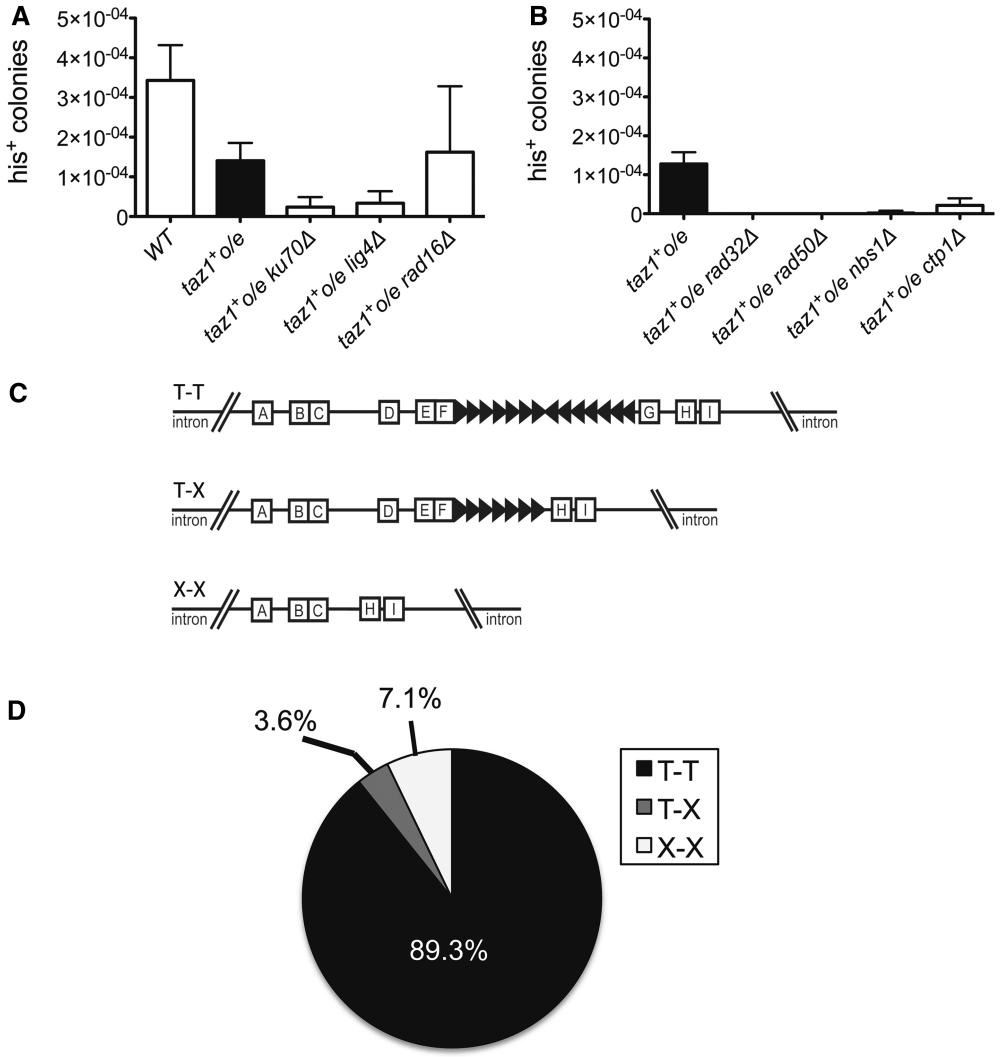

Figure 4. Spontaneous telomere fusions occur in unperturbed WT cells. (**A**) Frequency of fusions in WT, and *taz1*$^{+}$*o/e ku70*Δ, *taz1*$^{+}$*o/e lig4*Δ and *taz1*$^{+}$*o/e rad16*Δ strains. (**B**) Frequency of fusions in *taz1*$^{+}$*o/e rad32*Δ, *taz1*$^{+}$*o/e rad50*Δ, *taz1*$^{+}$*o/e nabs1*Δ and *taz1*$^{+}$*o/e ctp1*Δ strains. In (A) and (B), cells were plated in +HIS −LEU and −HIS −LEU media in triplicate. Percentage of his+ cells in the population was determined by dividing the number of his+ colonies by the total number of colonies. Error bars represent SEM of three independent experiments. The threshold of detection for (A) and (B) is 1×10^{-5} his+ colonies/total sample. (**C**) Classification of telomere fusion types. T-T (telomere to telomere): fusion junctions containing telomeric DNA from both ends. T-X: fusion junctions containing telomeric DNA on one end fused to a subtelomeric region. X-X: fusion junctions containing non-telomeric DNA. (**D**) Frequency of T-T, T-X and X-X fusions.

telomere shortening is more evident on terminator than on promoter proximal telomeres (Figure 5B). Median length of original telomere was half as long on the terminator proximal telomere (T Prom 101 bp and T Term 68 bp; IQR 75–149 bp and 18–103 bp, respectively). These differences could be explained by different affinity for telomerase, such that the T Term telomere is elongated only half of the times as the T Prom and thus erodes further acquiring a smaller steady state length.

Why are telomeres engaging in end-joining reactions? We reasoned that if one telomere would be critically short, it would engage in fusions with other telomeres independently of their size. Such was observed in budding yeast for fusions between a DSB and telomeres (24). However, this was not the case for our assay. By plotting telomere length of T Prom against T Term, we observed a positive correlation of sizes such that the longer the telomere was on one side, the longer it was on the other ($R^2 = 0.62$, $n = 28$; Figure 5C). Thus, the fusions observed cannot be explained by critical telomere shortening at one end of the mini-chromosome. Instead, telomeres appear to become stochastically deprotected, thereby undergoing NHEJ repair with neighbour telomeres.

DISCUSSION

Telomere erosion leading to critically short telomeres has been widely implicated in cancer (23,38–42). Studies using primary human cell lines have shown that telomeres engage in end fusions upon continuous erosion (23). Here, we show that unperturbed cells with seemingly functional telomeres can also engage in chromosome-end fusions. Telomere-to-telomere fusions are an undervalued

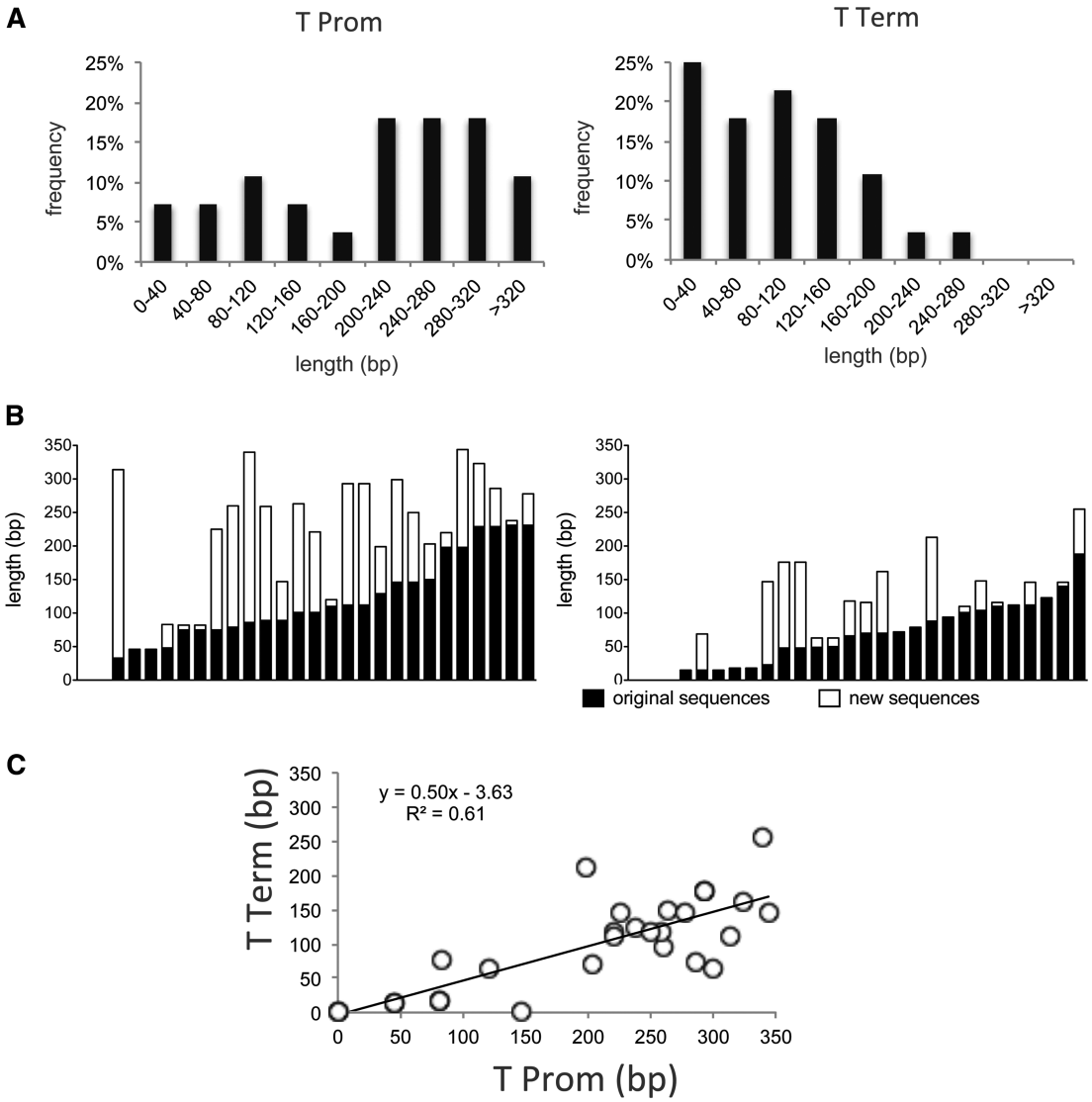

Figure 5. Mini-chromosomes undergo end fusions at half-sized telomere length. (**A**) Frequency of telomere fusions according to telomere length, at the promoter-proximal telomere (T Prom) and at the terminator-proximal telomere (T Term). (**B**) Telomere size of each telomere ($n = 28$). White bars represent originally cloned telomere sequences and black bars represent sequences added *in vivo*. (**C**) Pairwise telomere length distribution of mini-chromosome telomeres involved in fusions.

phenomenon owing to the difficulties in capturing and sequencing these events. This partially stems from the lack of quantitative positive detection assays (43–46). One such assay using an induced DSB in budding yeast provided an extremely low frequency of telomere-to-DSB fusion events [8.4×10^{-8} (24)]. Since we found far more frequent rate of telomere-to-telomere fusions (1.4×10^{-4}), it is tempting to speculate that spontaneous chromosome fusions may be a relevant trigger of genome instability and carcinogenesis. Consistent with this idea, recent evidence show telomere-to-telomere fusions in human breast carcinoma (42). The disparity in frequencies between our result and the one previously reported may simply reflect differences in the experimental setup. Unlike our assay, the telomere-to-DSB fusion assay relies on coinciding a DSB with transient telomere deprotection. Since G1 phase is predominant in budding yeast asynchronous cultures, a DSB generated during this stage may not be available in late S phase when telomeres are replicated and possibly deprotected. In contrast, our assay relies exclusively on transient telomere deprotection and these events occur synchronously by their own nature. Alternatively, the higher frequency of telomere fusions measured in our assay may simply reflect the artificial nature of the reporter construct. Our mini-chromosome possesses considerably short subtelomeric regions (ca. 80 bp) in comparison with chromosomal subtelomeres that encompass 10 kbp. Moreover, telomeres were introduced within an intron of a transcribed gene, a feature that may affect telomere protection.

The frequency of telomere fusions measured in our assay is likely to under-represent the total amount of those present in WT and *trt1*Δ mutants. Our system is unable to detect unproductive mini-chromosome-end

fusions, i.e. all those that fail to regenerate *his3*$^{+}$ expression. These could involve (i) the destruction of the coding sequence or intronic splice sites of the reporter gene; (ii) fusions between mini-chromosome and endogenous chromosome ends; (iii) fusions between mini-chromosomes that do not pair opposite ends or even (iv) the generation of linear *trt1*Δ survivors that continuously undergo homologous recombination (HR) at the chromosome ends.

Telomere-to-telomere fusions require the NHEJ pathway similar to what was found in *taz1*Δ, *rap1*$^{-}$ and TRF2$^{F/-}$ mutants (11,14,47,48). They also depend on the MRN complex, as was observed in TRF2$^{F/-}$ and *taz1*Δ fusions (49,50). Because in addition to MRN, fusions require the Ctp1 nuclease that is not present during G1 (51), these events are likely to occur later in the cell cycle, perhaps during DNA replication when telomeres are exposed. In fission yeast, *taz1*Δ telomeres are subject to HR during S/G2 phase of the cell cycle (52). However, dysfunctional telomeres can undergo NHEJ-mediated fusions in S/G2 when HR is compromised (11). We anticipate that upon DNA replication, telomere protection may occasionally be faulty. In late S phase, telomeres unfold to accommodate the DNA replication machinery causing momentary deprotection (53). This is corroborated by DNA damage responses being initiated every S phase as the replication fork reaches chromosome ends (16,54). Taz1 levels may also be limiting during this period to protect the newly duplicated telomeres. In support of this hypothesis, we observed that a strain with insufficient Taz1 undergoes telomere fusions at a higher frequency.

In contrast to unperturbed cells, chromosome fusions in the absence of telomerase were mediated by SSA/MMEJ repair. Choice of DSB repair may simply reflect telomere length and sequence. Although shelterin-protected longer telomeres prevent DNA-end 5′-resection required for SSA/MMEJ repair (55), ssDNA generated at critically short telomere inhibits NHEJ repair (49). Additionally, microhomologies are largely absent from telomere sequences involved in end-joining reactions [e.g. 5′-(TTAGGG)$_n$/(CCCTAA)$_n$-3′]. Previous work in *pot1*Δ and *trt1*Δ mutants showed extensive degradation of chromosome ends up to 13 kb (20). In contrast, our mini-chromosome ends in *trt1*Δ mutants fuse at specific pentanucleotide microhomologies contiguous to telomeres but not within the juxtaposed intronic region of *his3*$^{+}$, suggesting that intron sequences may be refractory to end-joining reaction. We observed that microhomologies were arranged in inverted repeats that, when resected, could fold back and engage in DNA hairpin formation. Fusions in *trt1*Δ mutants require the MRN complex and Ctp1. Thus, hairpins may serve as stabilizing structures for eroding DNA ends, which are subsequently processed by MRN/Ctp1 and captured in end-fusion reactions (36,56). MRN was similarly required for chromosome fusions involving critically short telomeres in Arabidopsis and human cells (45,57), and telomerase RNA mutants in budding yeast (58). Alternatively, hairpins formed during DNA replication can lead to end-joining reactions (59,60). Recent evidence shows that DNA replication plays a role in chromosome-end fusions in *Caenorhabditis elegans* (61). However, we were unable to detect fusions involving pentanucleotide repeats in WT cells, suggesting they require telomere resection prior to fusion. Future studies will reveal the role of these naturally occurring subtelomeric DNA microhomologies in telomere fusions.

Our mini-chromosome allowed us to assess end-to-end fusions in several distinct genetic backgrounds. Furthermore, we established that there are two distinct pathways that generate chromosome-end fusions, which are determined by the mechanism of uncapping, and that both are likely to be of importance in the development of genome instability and cancer.

SUPPLEMENTARY DATA

Supplementary Data are available at NAR Online: Supplementary Table 1 and Supplementary Figures 1–6.

ACKNOWLEDGEMENTS

We thank members of our laboratory for helpful discussions. We are indebted to Julie Cooper for support at the initial stages of this work and for kindly providing the α-Taz1 antibody. We are grateful to Kurt Runge, Karel Riha and Kazunori Tomita for critically reading our manuscript. Miguel Godinho Ferreira is an HHMI international early career scientist.

FUNDING

Portuguese Fundação para a Ciência e Tecnologia [PTDC/SAU-OBD/66438/2006, SFRH/BD/62050/2009]; Association for International Cancer Research [Ref: 06-396]. Funding for open access charge: Portuguese Fundação para a Ciência e Tecnologia [PTDC/SAU-OBD/66438/2006]

Conflict of interest statement. None declared.

REFERENCES

1. Stewart,J.A., Chaiken,M.F., Wang,F. and Price,C.M. (2012) Maintaining the end: roles of telomere proteins in end-protection, telomere replication and length regulation. *Mutat. Res.*, **730**, 12–19.
2. Cooper,J.P., Nimmo,E.R., Allshire,R.C. and Cech,T.R. (1997) Regulation of telomere length and function by a Myb-domain protein in fission yeast. *Nature*, **385**, 744–747.
3. Hackett,J.A., Feldser,D.M. and Greider,C.W. (2001) Telomere dysfunction increases mutation rate and genomic instability. *Cell*, **106**, 275–286.
4. Sfeir,A. and de Lange,T. (2012) Removal of shelterin reveals the telomere end-protection problem. *Science*, **336**, 593–597.
5. de Lange,T. (2005) Shelterin: the protein complex that shapes and safeguards human telomeres. *Genes Dev.*, **19**, 2100–2110.
6. Martínez,P. and Blasco,M.A. (2010) Role of shelterin in cancer and aging. *Aging Cell*, **9**, 653–666.
7. Lingner,J., Cooper,J.P. and Cech,T.R. (1995) Telomerase and DNA end replication: no longer a lagging strand problem? *Science*, **269**, 1533–1534.
8. Blackburn,E.H. and Greider,C.W. (1985) Identification of a specific telomere terminal transferase activity in Tetrahymena extracts. *Cell*, **43**, 405–413.

9. Blackburn,E.H., Greider,C.W., Henderson,E., Lee,M.S., Shampay,J. and Shippen-Lentz,D. (1989) Recognition and elongation of telomeres by telomerase. *Genome*, **31**, 553–560.
10. Nakamura,T.M., Morin,G.B., Chapman,K., Weinrich,S.L., Andrews,W., Lingner,J., Harley,C.B. and Cech,T.R. (1997) Telomerase catalytic subunit homologs from fission yeast and human. *Science*, **277**, 955–959.
11. Ferreira,M.G. and Cooper,J.P. (2001) The fission yeast Taz1 protein protects chromosomes from Ku-dependent end-to-end fusions. *Mol. Cell*, **7**, 55–63.
12. Miller,K.M., Ferreira,M.G. and Cooper,J.P. (2005) Taz1, Rap1 and Rif1 act both interdependently and independently to maintain telomeres. *EMBO J.*, **24**, 3128–3135.
13. Smogorzewska,A., Karlseder,J., Holtgreve-Grez,H., Jauch,A. and de Lange,T. (2002) DNA ligase IV-dependent NHEJ of deprotected mammalian telomeres in G1 and G2. *Curr. Biol.*, **12**, 1635–1644.
14. Pardo,B. and Marcand,S. (2005) Rap1 prevents telomere fusions by nonhomologous end joining. *EMBO J.*, **24**, 3117–3127.
15. Teixeira,M.T., Arneric,M., Sperisen,P. and Lingner,J. (2004) Telomere length homeostasis is achieved via a switch between telomerase-extendible and-nonextendible states. *Cell*, **117**, 323–335.
16. Verdun,R.E. and Karlseder,J. (2006) The DNA damage machinery and homologous recombination pathway act consecutively to protect human telomeres. *Cell*, **127**, 709–720.
17. Martín,V., Du,L.L., Rozenzhak,S. and Russell,P. (2007) Protection of telomeres by a conserved Stn1-Ten1 complex. *Proc.Natl. Acad. Sci.*, **104**, 14038–14043.
18. Wang,X. and Baumann,P. (2008) Chromosome fusions following telomere loss are mediated by single-strand annealing. *Mol. Cell*, **31**, 463–473.
19. Decottignies,A. (2007) Microhomology-mediated end joining in fission yeast is repressed by Pku70 and relies on genes involved in homologous recombination. *Genetics*, **176**, 1403–1415.
20. Nakamura,T.M., Cooper,J.P. and Cech,T.R. (1998) Two modes of survival of fission yeast without telomerase. *Science*, **282**, 493–496.
21. Rai,R., Zheng,H., He,H., Luo,Y., Multani,A., Carpenter,P.B. and Chang,S. (2010) The function of classical and alternative non-homologous end-joining pathways in the fusion of dysfunctional telomeres. *EMBO J.*, **29**, 2598–2610.
22. Hemann,M.T., Strong,M.A., Hao,L.Y. and Greider,C.W. (2001) The shortest telomere, not average telomere length, is critical for cell viability and chromosome stability. *Cell*, **107**, 67–77.
23. Capper,R., Britt-Compton,B., Tankimanova,M., Rowson,J., Letsolo,B., Man,S., Haughton,M. and Baird,D.M. (2007) The nature of telomere fusion and a definition of the critical telomere length in human cells. *Genes Dev.*, **21**, 2495–2508.
24. DuBois,M.L., Haimberger,Z.W., McIntosh,M.W. and Gottschling,D.E. (2002) A quantitative assay for telomere protection in Saccharomyces cerevisiae. *Genetics*, **161**, 995–1013.
25. Sugawara,N. (1989) *Thesis*. Harvard University, Cambridge, MA.
26. Nimmo,E.R., Cranston,G. and Allshire,R.C. (1994) Telomere-associated chromosome breakage in fission yeast results in variegated expression of adjacent genes. *EMBO J.*, **13**, 3801.
27. Moreno,S., Klar,A. and Nurse,P. (1991) Molecular genetic analysis of fission yeast Schizosaccharomyces pombe. *Methods Enzymol.*, **194**, 795.
28. Bähler,J., Wu,C., Longtine,M., Shah,N., McKenzie,A. III, Steever,A.B., Wach,A., Philippsen,P. and Pringle,J.R. (1998) Heterologous modules for efficient and versatile PCR-based gene targeting in Schizosaccharomyces pombe. *Yeast*, **14**, 943–951.
29. Sato,M., Dhut,S. and Toda,T. (2005) New drug-resistant cassettes for gene disruption and epitope tagging inSchizosaccharomyces pombe. *Yeast*, **22**, 583–591.
30. Kimura,M., Stone,R.C., Hunt,S.C., Skurnick,J., Lu,X., Cao,X., Harley,C.B. and Aviv,A. (2010) Measurement of telomere length by the Southern blot analysis of terminal restriction fragment lengths. *Nature Protocols*, **9**, 1596–1607.
31. Beach,D. and Nurse,P. (1981) High-frequency transformation of the fission yeast Schizosaccharomyces pombe. *Nature*, **290**, 140–142.
32. Wiley,E.A. and Zakian,V.A. (1995) Extra telomeres, but not internal tracts of telomeric DNA, reduce transcriptional repression at Saccharomyces telomeres. *Genetics*, **139**, 67–79.
33. Runge,K.W. and Zakian,V.A. (1989) Introduction of extra telomeric DNA sequences into Saccharomyces cerevisiae results in telomere elongation. *Mol. Cell. Biol.*, **9**, 1488–1497.
34. Baumann,P. and Cech,T.R. (2000) Protection of telomeres by the Ku protein in fission yeast. *Mol. Biol. Cell*, **11**, 3265–3275.
35. Lobachev,K.S., Gordenin,D.A. and Resnick,M.A. (2002) The Mre11 complex is required for repair of hairpin-capped double-strand breaks and prevention of chromosome rearrangements. *Cell*, **108**, 183–193.
36. Lengsfeld,B.M., Rattray,A.J., Bhaskara,V., Ghirlando,R. and Paull,T.T. (2007) Sae2 Is an endonuclease that processes hairpin DNA cooperatively with the Mre11/Rad50/Xrs2 complex. *Mol. Cell*, **28**, 638–651.
37. Manolis,K.G., Nimmo,E.R., Hartsuiker,E., Carr,A.M., Jeggo,P.A. and Allshire,R.C. (2001) Novel functional requirements for non-homologous DNA end joining in Schizosaccharomyces pombe. *EMBO J.*, **20**, 210–221.
38. Artandi,S.E., Chang,S., Lee,S.L., Alson,S., Gottlieb,G.J., Chin,L. and DePinho,R.A. (2000) Telomere dysfunction promotes non-reciprocal translocations and epithelial cancers in mice. *Nature*, **406**, 641–644.
39. Shay,J.W. and Wright,W.E. (2011) Role of telomeres and telomerase in cancer. *Semin. Cancer Biol.*, **21**, 349–353.
40. Letsolo,B.T., Rowson,J. and Baird,D.M. (2010) Fusion of short telomeres in human cells is characterized by extensive deletion and microhomology, and can result in complex rearrangements. *Nucleic Acids Res.*, **38**, 1841–1852.
41. Lin,T.T., Letsolo,B.T., Jones,R.E., Rowson,J., Pratt,G., Hewamana,S., Fegan,C., Pepper,C. and Baird,D.M. (2010) Telomere dysfunction and fusion during the progression of chronic lymphocytic leukemia: evidence for a telomere crisis. *Blood*, **116**, 1899–1907.
42. Tanaka,H., Abe,S., Huda,N., Tu,L., Beam,M.J., Grimes,B. and Gilley,D. (2012) Telomere fusions in early human breast carcinoma. *Proc. Natl Acad. Sci.*, **109**, 14098–14103.
43. McEachern,M.J., Iyer,S., Fulton,T.B. and Blackburn,E.H. (2000) Telomere fusions caused by mutating the terminal region of telomeric DNA. *Proc. Natl. Acad. Sci.*, **97**, 11409–11414.
44. Mieczkowski,P.A., Mieczkowska,J.O., Dominska,M. and Petes,T.D. (2003) Genetic regulation of telomere-telomere fusions in the yeast Saccharomyces cerevisae. *Proc. Natl. Acad. Sci.*, **100**, 10854–10859.
45. Heacock,M., Spangler,E., Riha,K., Puizina,J. and Shippen,D.E. (2004) Molecular analysis of telomere fusions in Arabidopsis: multiple pathways for chromosome end-joining. *EMBO J.*, **23**, 2304–2313.
46. Lowden,M.R., Meier,B., Lee,T.W.s., Hall,J. and Ahmed,S. (2008) End joining at caenorhabditis elegans telomeres. *Genetics*, **180**, 741–754.
47. Bae,N.S. and Baumann,P. (2007) A RAP1/TRF2 Complex inhibits nonhomologous end-joining at human telomeric DNA ends. *Mol. Cell*, **26**, 323–334.
48. Muraki,K., Nyhan,K., Han,L. and Murnane,J.P. (2012) Mechanisms of telomere loss and their consequences for chromosome instability. *Front. Oncol.*, **2**, 135.
49. Dimitrova,N. and de Lange,T. (2009) Cell cycle-dependent role of MRN at dysfunctional telomeres: ATM signaling-dependent induction of nonhomologous end joining (NHEJ) in G1 and resection-mediated inhibition of NHEJ in G2. *Mol. Cell. Biol.*, **29**, 5552–5563.
50. Reis,C.C., Batista,S. and Ferreira,M.G. (2012) The fission yeast MRN complex tethers dysfunctional telomeres for NHEJ repair. *EMBO J.*, 1–11.
51. Limbo,O., Chahwan,C., Yamada,Y., de Bruin,R.A.M., Wittenberg,C. and Russell,P. (2007) Ctp1 is a cell-cycle-regulated protein that functions with Mre11 complex to control double-strand break repair by homologous recombination. *Mol. Cell*, **28**, 134–146.

52. Rog,O., Miller,K.M., Ferreira,M.G. and Cooper,J.P. (2009) Sumoylation of RecQ helicase controls the fate of dysfunctional telomeres. *Mol. Cell*, **33**, 559–569.
53. Verdun,R.E. and Karlseder,J. (2007) Replication and protection of telomeres. *Nature*, **447**, 924–931.
54. Moser,B.A., Subramanian,L., Chang,Y.T., Noguchi,C., Noguchi,E. and Nakamura,T.M. (2009) Differential arrival of leading and lagging strand DNA polymerases at fission yeast telomeres. *EMBO J.*, **28**, 810–820.
55. Pitt,C.W. and Cooper,J.P. (2010) Pot1 inactivation leads to rampant telomere resection and loss in one cell cycle. *Nucleic Acids Res.*, **38**, 6968–6975.
56. Helmink,B.A., Tubbs,A.T., Dorsett,Y., Bednarski,J.J., Walker,L.M., Feng,Z., Sharma,G.G., McKinnon,P.J., Zhang,J., Bassing,C.H. *et al.* (2010) H2AX prevents CtIP–mediated DNA end resection and aberrant repair in G1-phase lymphocytes. *Nature*, **469**, 245–249.
57. Tankimanova,M., Capper,R., Letsolo,B.T., Rowson,J., Jones,R.E., Britt-Compton,B., Taylor,A.M. and Baird,D.M. (2012) Mre11 modulates the fidelity of fusion between short telomeres in human cells. *Nucleic Acids Res.*, **40**, 2518–2526.
58. Chan,S.W.L. and Blackburn,E.H. (2003) Telomerase and ATM/Tel1p protect telomeres from nonhomologous end joining. *Mol. Cell*, **11**, 1379–1387.
59. Murnane,J.P. (2012) Telomere dysfunction and chromosome instability. *Mutat. Res.*, **730**, 28–36.
60. Haber,J.E. and Debatisse,M. (2006) Gene amplification: yeast takes a turn. *Cell*, **125**, 1237–1240.
61. Lowden,M.R., Flibotte,S., Moerman,D.G. and Ahmed,S. (2011) DNA synthesis generates terminal duplications that seal end-to-end chromosome fusions. *Science*, **332**, 468–471.